Optics & Laser Technology 66 (2015) 89–97

Contents lists available at ScienceDirect

Optics & Laser Technology

journal homepage: www.elsevier.com/locate/optlastec

Review

Swarm intelligence for atmospheric compensation in free space optical communication—Modified shuffled frog leaping algorithm

Zhaokun Li [a], Jingtai Cao [a,b], Xiaohui Zhao [a,*], Wei Liu [a]

[a] College of Communication Engineering, Jilin University, 5372 Nanhu Road, Changchun 130012, PR China
[b] Changchun Institute of Optics, Fine Mechanics and Physics, Chinese Academy of Sciences, 3888 Nanhu Road, Changchun 130033, PR China

ARTICLE INFO

Article history:
Received 17 June 2014
Received in revised form
19 August 2014
Accepted 20 August 2014
Available online 16 September 2014

Keywords:
Free space optical communication
Swarm intelligence
Coupling efficiency

ABSTRACT

A conventional adaptive optics (AO) system is widely used to compensate atmospheric turbulence in free space optical (FSO) communication systems, but wavefront measurements based on phase-conjugation principle are not desired under strong scintillation circumstances. In this study we propose a novel swarm intelligence optimization algorithm, which is called modified shuffled frog leaping algorithm (MSFL), to compensate the wavefront aberration. Simulation and experiments results show that MSFL algorithm performs well in the atmospheric compensation and it can increase the coupling efficiency in receiver terminal and significantly improve the performance of the FSO communication systems.

Contents

1. Introduction

A free space optical (FSO) communication system is widely used among the telecommunication community for both space and ground wireless link and last-mile applications [1] due to its unregulated spectrum, large bandwidth potential, relative low power requirement, low BER and ease of redeployment. However, atmospheric turbulence will bring phase disturbances along propagation paths that are manifested as intensity fluctuation (scintillation), beam wandering and beam broadening at the receiver, leading to significant decrease of coupling efficiency at the receiving terminal [2], which influences the stability and reliability of the FSO communication systems [3]. An adaptive optical (AO) system is an effective method to improve laser beam quality by correcting the wavefront aberration; it has already made great achievements [4–9]. In the conventional AO system, a deformable

* Corresponding author.
E-mail address: xhzhao@jlu.edu.cn (X. Zhao).

http://dx.doi.org/10.1016/j.optlastec.2014.08.012
0030-3992/

mirror (DM) is used to compensate the phase distortion. Generally, the Shack Hartmann wavefront sensor (S–H sensor) [10] measures the optical phase deviations of the incoming wavefront. DM generates a wavefront phase to compensate the phase aberration based on the phase conjugation theory [11,12].

Strong scintillation results in very difficult measurement for the wavefront aberration, and the conventional AO system based on wavefront measurement cannot work normally [13]; thus control of the wavefront correctors in the AO system can be conducted by using recently developed control algorithm based on optimization of a system performance metric, such as stochastic parallel gradient descent (SPGD) algorithm. Although the concept of wavefront control without wavefront measurement has been considered in the early stages of AO technology development [14–16], it has been largely disregarded because of the rather low control bandwidth that could be achieved even with a multi-dithering control technique [17,18]. But this situation has been largely different today because of the development of several novel technologies, for example, some efficient control algorithms whose implementation with parallel processing hard-ware, and the emergence of high-bandwidth wavefront correctors are based on microelectromechanical systems (MEMSs) [19].

Different from the traditional intelligent optimization algorithms, e.g. SPGD algorithm [13], swarm intelligence algorithms are novel optimized algorithms which imitate the natural biological group behaviors. Swarms are the systems that consist of many individuals which are organized and coordinated by principles of decentralized control, indirect communication, and self-organization. An interesting phenomenon of swarms is that collective swarm behavior can lead to a change on a global scale even one individual has only a restricted view. Examples for such collective behaviors are the nest building of ants or the coordinated movement of fish swarm [20]. The basic idea of swarm intelligence algorithms is using the solutions in the searching space as the individuals in nature. Take the "evolution and foraging process" as an analogy of the process of random search, the objective functions are equal to adaptive capability to natural environment. Consequently, based on the selection mechanism, replace a bad individual by a better one, make the individuals closer to the optimized solution, it can be considered as the iteration process of the random searching. It has been used in many fields such as artificial intelligence, robots and data analysis.

In this paper, we analyze the performance of the modified shuffled frog leaping (MSFL) algorithm in the FSO system. Particle swarm optimization (PSO) algorithm and SPGD algorithm are also simply introduced as comparisons. Related theoretical analysis and simulations indicate that MSFL algorithm increases the coupling efficiency at the receiving terminal, improve the performance of the FSO communication system, and some detailed differences between these algorithms due to their search strategies are worth researching. Because of the characters of MSFL algorithm, the effect of different individual-numbers and different group-numbers in MSFL is also important to the FSO system.

This paper is organized as follows: Section 2 provides the models of the FSO communication system, the sensorless AO system and DM. Section 3 analyses of MSFL algorithm related to the other two algorithms (PSO and SPGD) and their work principles in the FSO communication system is given. In Section 4, some simulations and experiments are carried out to show the comparisons of the improved performance of MSFL with other algorithms in the FSO communication system. In addition, the effect of different individual-numbers and group-numbers on the FSO system is analyzed. Finally, conclusions for this paper are given in Section 5.

2. System model

2.1. The FSO communication system model

The functional block diagram of the FSO communication system is shown in Fig. 1 [2].

The laser point source emits a Gaussian laser beam. The atmospheric disturbances reduce the fiber coupling efficiency at the receiver; the communication quality is seriously affected. The sensorless AO system is used here to compensate the wavefront aberrations. After compensation for the wavefront aberration, the laser beam is

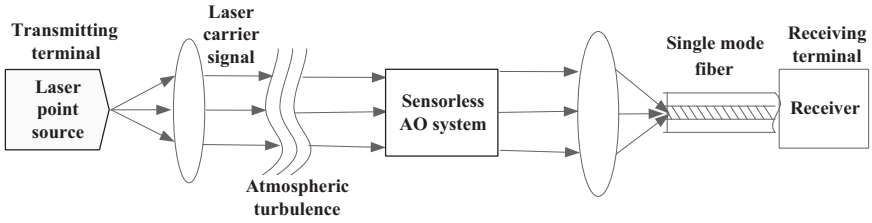

Fig. 1. Functional block diagram of the FSO system.

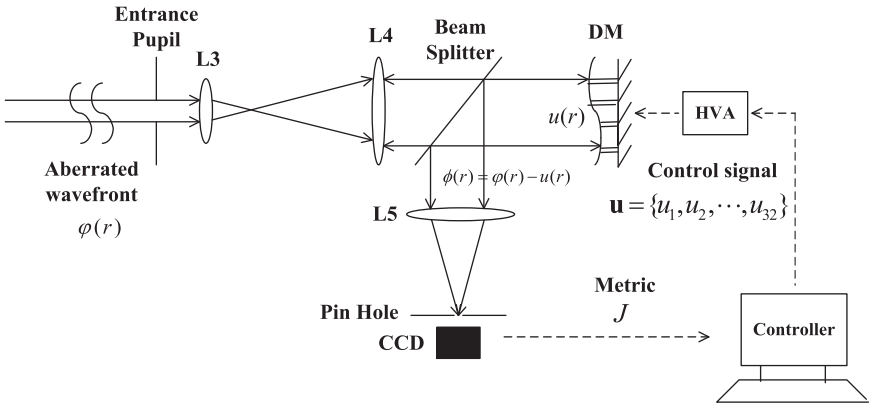

Fig. 2. Block diagram of simulation.

coupled into a single mode fiber. The coupling efficiency is the main metric, higher coupling efficiency means better performance in the system. Based on the theoretical analysis and the simulations, the coupling efficiency can be significantly improved.

2.2. The sensorless AO system model

The theoretical block diagram of wavefront aberration compensation by DM is shown in Fig. 2. $\varphi(r)$ is the incident wavefront aberration, $u(r)$ is the compensation phase, $\phi(r)=\varphi(r)-u(r)$ is the residual phase, and J is the performance metric. The AO system mainly uses DM to correct the wavefront aberration $\varphi(r)$, while a CCD is used to record the intensity on focal plane. Swarm intelligence algorithm produces control signals $\mathbf{u}=\{u_1,u_2,\cdots,u_{32}\}$ for the DM according to the performance metric J.

2.3. The DM model

The normalized layout of 32-element DM actuators is shown in Fig. 3.

We approximate the influence function of DM by the Gaussian Model

$$S_j(x,y)=\exp\left\{\ln\omega\left[\frac{1}{d}\sqrt{(x-x_j)^2+(y-y_j)^2}\right]^{\alpha}\right\} \tag{1}$$

where ω is the coupling coefficient determined by the sizes of electrode actuators and the DM. (x_j,y_j) is the center coordinate of the jth actuator. d is the normalized interval between the adjacent actuators, and α is the Gaussian index. The phase compensation $u(x,y)$ generated by the deformable mirror is given by

$$u(x,y)=\sum_{j=1}^{32} v_j S_j(x,y) \tag{2}$$

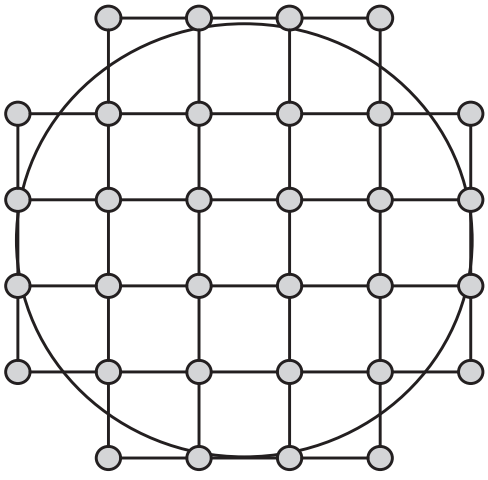

Fig. 3. Layout of 32-element deformable mirrors actuators (filled circles).

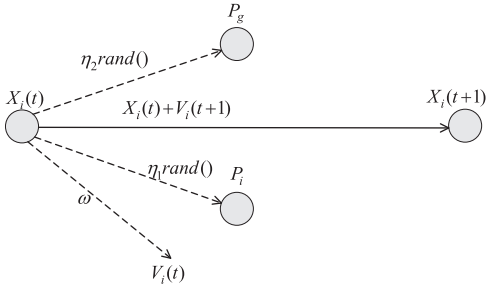

Fig. 4. Sketch of PSO algorithm.

where v_j is the jth voltage of the actuators. We can see that the numeral relationship between the phase aberration generated by the DM and voltages applied on the actuators is linear.

3. Analysis of swarm intelligence in the FSO communication system

3.1. The fitness

As for using swarm intelligence algorithms in the FSO communication system, the first step is to initialize N solutions. They are all 32-demension vectors, every component in the vectors means the voltage applied on the actuator. In this paper, they are evenly distributed in the range of the maximum possible voltage. Then we continuously update these solutions to make them closer to an optimum solution. The objective function in these algorithms is based on the root-mean-square (RMS) value of the residual phase aberration

$$\text{fitness}=\frac{1}{RMS} \tag{3}$$

where

$$RMS=\iint_S(\varphi(r)-\overline{\varphi(r)})^2 r\cdot dr=\iint_S[(\varphi(r)+u(r))-\overline{(\varphi(r)+u(r))}]^2 r\cdot dr \tag{4}$$

where $\varphi(r)$ is the initial wavefront aberration, $u(r)$ is the compensation phase that can be obtained by Eq. (2), $\phi(r)=\varphi(r)+u(r)$ is the residual phase, and S is the normalized circle of DM.

In the following study, the better solution (or better location) means its better (or higher) fitness.

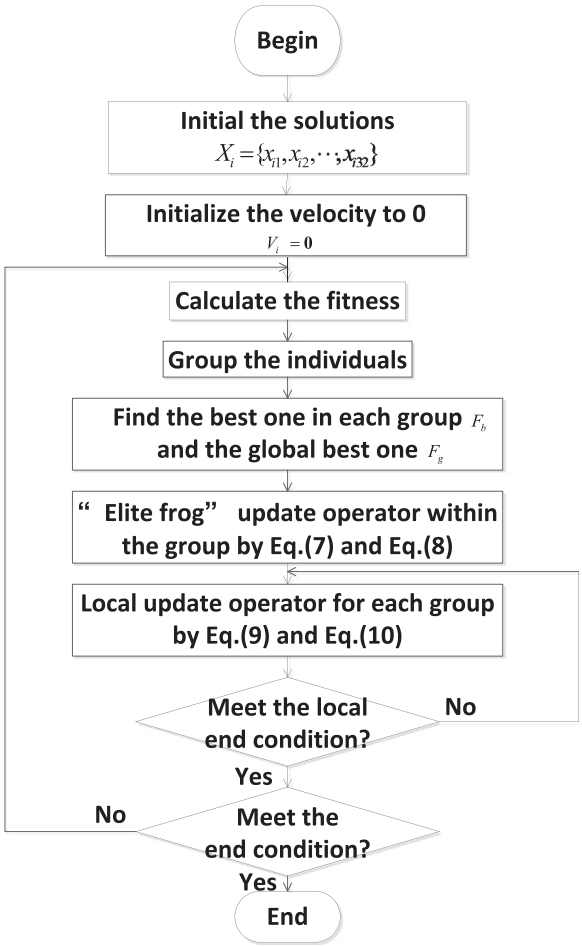

Fig. 5. MSFL algorithm flowchart.

3.2. PSO algorithm

Simply introduce PSO [21,22] because it makes sense in our subject. The particle swarm searches in n-dimensional space consisting of N particles $X=\{X_1,X_2,\cdots,X_N\}$, each location is a solution $X_i=\{x_{i1},x_{i2},\cdots,x_{in}\}$, the particle continually changes position X_i to get a better solution. Each particle remembers the best position P_i it experienced and the best solution P_g within the whole group. Each particle has a velocity $V_i=\{v_{i1},v_{i2},\cdots,v_{in}\}$, the update of X_i is

$$V_i(t+1)=\omega\cdot V_i(t)+\eta_1\cdot \text{rand}()\cdot(P_i-X_i(t))+\eta_2\cdot \text{rand}()\cdot(P_g-X_i(t)) \quad (5)$$

$$X_i(t+1)=X_i(t)+V_i(t+1) \quad (6)$$

where $V_i(t)$ is the velocity in the tth iteration, ω is the inertia weight, η_1 and η_2 are the acceleration constants, rand() is a random number between 0 and 1. The meaning is shown in Fig. 4. As PSO has rapid convergence speed and is easy to implement and it has been widely applied in many aspects. However, the precision of PSO algorithm is low, and it is easy to produce premature convergence [23].

3.3. MSFL algorithm

SFL algorithm is a novel heuristic search method based on swarm intelligence. It imitates the foraging of the frogs in nature, uses the collaboration and information interaction for reference to solve the optimization problems. It also uses the memes grouping algorithm to imitate the bunching of the frogs, implements leaping behavior by clustering and regrouping. By information sharing and exchange mechanism between the individuals, the heuristic search starts to find optimal solution. Because of the high efficient parallel computing and excellent global searching capability, SFL algorithm is used in many fields. However, the drawback of slow convergence like AFS also exists. By introducing "velocity–displacement" model of PSO to SFL algorithm, the corresponding three behavior operators of the MSFL is described below.

(1) *Grouping operation*. In this operation, MSFL algorithm initializes a set of solutions (the initial frogs), sorts the results in descending order by their fitness, and puts them in the different groups. The grouping method is as follows: sort the N frogs in descending order by their fitness and divide them into m groups, the 1st frog in the 1st group, the 2nd frog in the 2nd group, the mth frog in the mth group; the $m+1$ th frog in the 1st group, the $m+2$th frog in the 2nd group,…, until all the frogs are in the groups.
With "elite frog" update operator and local update operator, the best frog F_g is updated.

(2) *"Elite frog" update operator.* The biggest change occurs in this operator (it does not exist in traditional SFL). The best frog F_b in each group (we call it the "elite frog") is updated by

$$V_{bnext}=\omega\cdot V_b+\eta_1\cdot \text{rand}()\cdot(P_b-X_b)+\eta_2\cdot \text{rand}()\cdot(F_g-X_b) \quad (7)$$

$$X_{bnext}=X_b+V_{bnext} \quad (8)$$

where F_g is the global best frog, P_b is the best position the "Elite frog" experienced. V_b is the current velocity, and V_{bnext} is the updated velocity. X_b is the current location and X_{bnext} is the new location.

(3) *Local update operator*. In each group, we use the best frog F_b to update each position X_i

$$V_{inext}=\omega\cdot V_i+\eta_1\cdot \text{rand}()\cdot(P_i-X_i)+\eta_2\cdot \text{rand}()\cdot(F_b-X_i) \quad (9)$$

$$X_{inext}=X_i+V_{inext} \quad (10)$$

where P_i is the best position the frog has experienced.

MSFL algorithm transmits information by three operators: grouping; local update; "elite frog" update. It combines the local information and global information. Local searching leads to the local exchange, and mixed strategy brings the information exchange between the

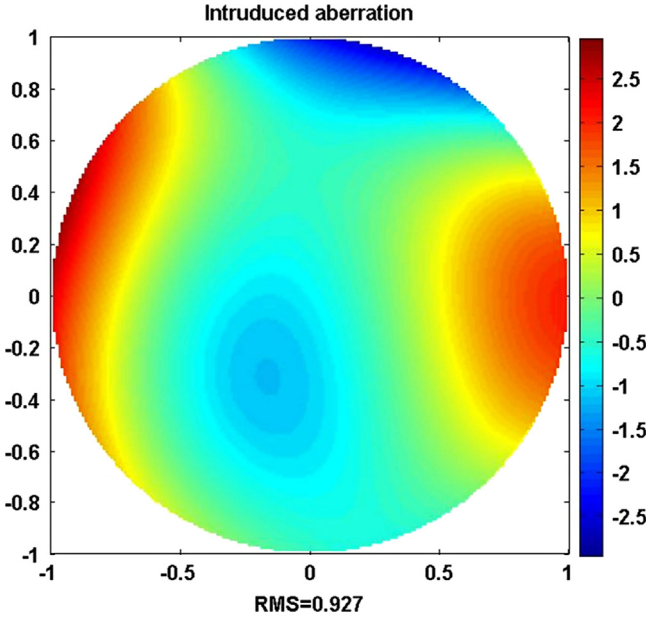

Fig. 6. Introduced wavefront aberration.

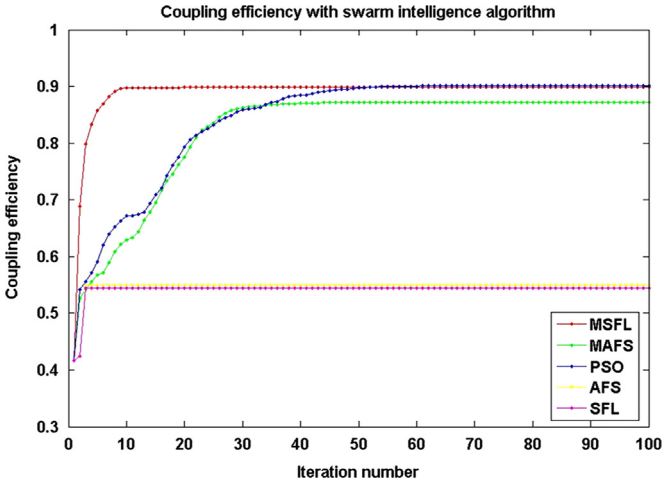

Fig. 7. Coupling efficiency with swarm intelligence algorithm.

Table 1
Zernike coefficients of introduced wavefront aberration.

Zernike order	3rd order	4th order	5th order	6th order	7th order	8th order	9th order	10th order
Zernike coefficient	1.30	0.65	−0.40	0.32	−0.45	−0.30	0.25	−0.15

groups. Due to the influence of group best solution and the global best solution, each frog has a mechanism of learning from other frogs. The update of each frog position is conducive to the improvement of the fitness of every group. After clustering, the fitness of the whole frogs is also improved, so the frogs are closer to the global best solution. In this way (information exchange and sharing), MSFL algorithm will not be trapped in the local optimum and has a high speed in convergence. The flow chart is shown in Fig. 5. AFS algorithm is a new method based on animal behaviors and the typical application of behaviorism artificial intelligence, each fish selects a behavior (from foraging, bunching and rear-ending) to discover surroundings and improves current position. It normally converges slowly when the search process is in a high dimensional space, the "velocity–displacement" model can be introduced to AFS algorithm, too.

3.4. Comparison of MSFL and SPGD

SPGD algorithm is implemented in application-specific analog VLSI controller chips with a PC as the supervisory controller [13]. The VLSI chips generate a set of statistically independent control parameter perturbation $\{\delta u_j^{(n)}\}$ in parallel for all N control voltages ($j=1,2,...,32$) at each iteration n. All perturbations have the same absolute values ε but pseudorandom signs (Bernoulli distribution, $\delta u=\pm\varepsilon$) with a probability of 0.5 for both positive and negative values. After application of the control voltage perturbations to the DM, the system measures a perturbed metric value $J_+^{(n)}$. Then the signs of all perturbation voltages are inverted and the corresponding value $J_-^{(n)}$ is measured, i.e.

$$J_\pm^{(n)}=J[u_1^{(n)}\pm\delta u_1^{(n)},\ldots,u_j^{(n)}\pm\delta u_j^{(n)},\ldots,u_N^{(n)}\pm\delta u_N^{(n)}] \tag{11}$$

The control voltages are then updated according to the rule

$$u_j^{(n+1)}=u_j^{(n)}+\gamma[J_+^{(n)}-J_-^{(n)}]\mathrm{sign}[\delta u_j^{(n)}] \tag{12}$$

where the update coefficient γ might be fixed or variable and controlled by a supervisory control loop. In the experiments here we adjusted γ to be approximately reciprocal to the actual value of the metric, $\gamma=\gamma_0/(J+C)$, where the constant $C>0$ to avoid too large control voltage updates if J comes close to 0. SPGD has a good convergence value but a slow convergence speed (compared with the MSFL). If we use the parallel processing technology (the

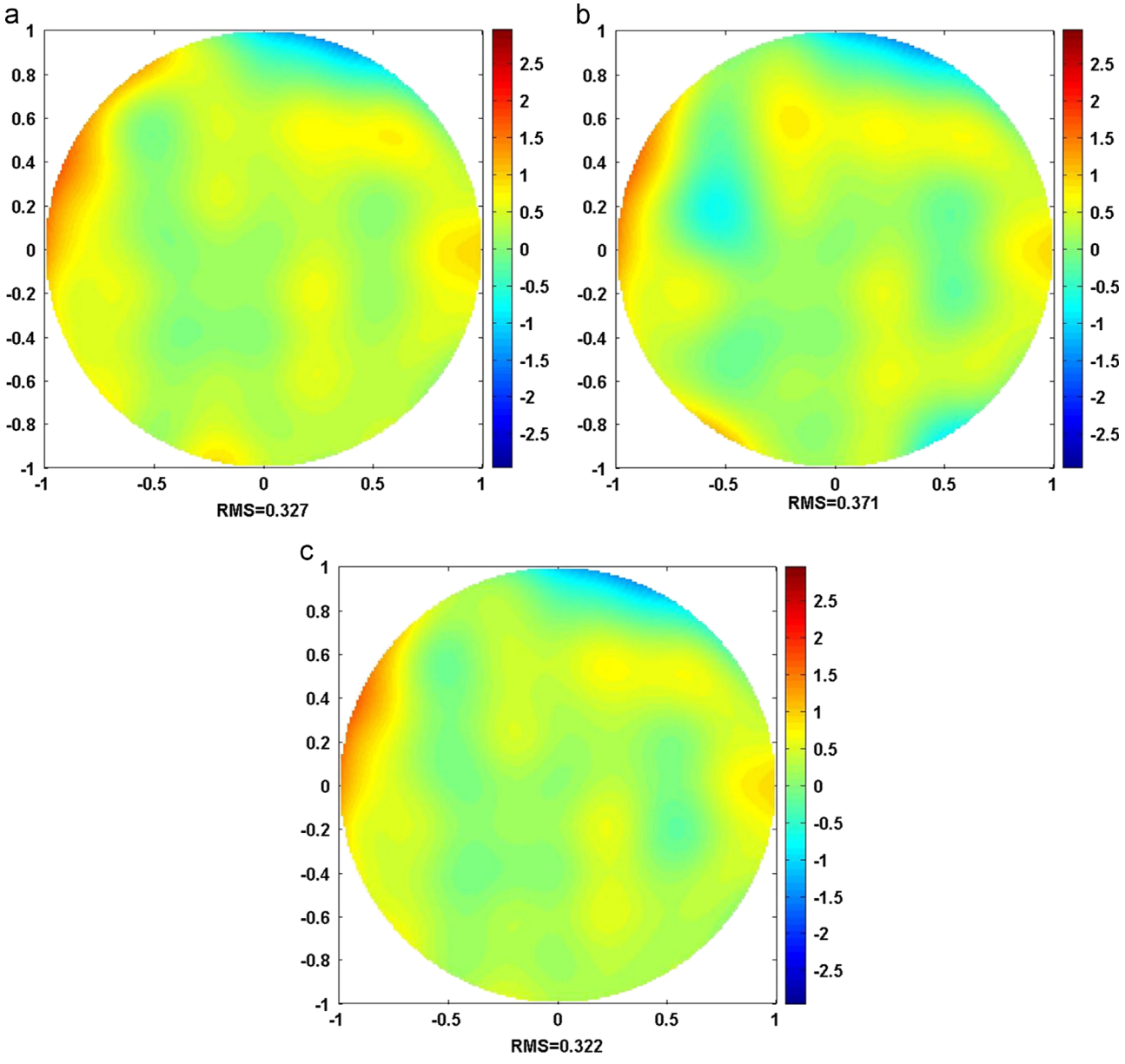

Fig. 8. Residual wavefront aberrations with MSFL, MAFS and PSO.

simplest way is using many computing elements that work simultaneously) to reduce the computation pressure, MSFL will offer a better performance on compensation of the phase aberration. The following numeral simulations will present some results.

3.5. Analysis of the performance in the FSO communication system

The goal of a conventional adaptive optics system is to minimize the residual phase aberrations after the incoming wave passes the deformable mirror. This corresponds to the maximization of the Strehl Ratio (*ST*), which is defined as the ratio of the actual maximum intensity of the zero order diffraction spot and its theoretical upper limitation for an undistorted wave.

Generally, the received laser signals are coupled into a single mode fiber, so the coupling efficiency of single mode fiber, defined as the ratio of the average power coupled into the fiber to the average power in the receiver aperture plane [24], has significant influence on the performance of the FSO system. The coupling efficiency can be expressed as

$$J \propto \frac{\left| \iint A_f(r) M_0^*(r) d^2 r \right|^2}{\iint A_f(r) A_f^*(r) d^2 r \times \iint M_0(r) M_0^*(r) d^2 r} \tag{13}$$

where $A_f(r)$ is the Fourier transform of single-mode fiber optical field, $M_0(r)$ is the incident optical field in the focal plane, $A_f(r)$ and $M_0(r)$ are complex quantities. Since Eq. (12) is too complex to calculate, we apply

$$ST \propto |A_f(r_0)|^2 \tag{14}$$

to simplify the average coupling efficiency [24,25], where r_0 is the desired on-axis location of the center of the fiber. Assume that the wavefront phase aberration satisfies Gaussian distribution, then *ST* can be estimated by variance as follows:

$$ST \propto \exp\left(-RMS^2\right) \tag{15}$$

with the increase of the coupling efficiency, more energy is coupled into the single mode fiber. When RMS^2 is close to 0, we can get a more simple formula

$$ST \propto 1 - RMS^2 \tag{16}$$

In practice, pixel size of CCD camera approximately equals to the fiber diameter; hence *ST* is expressed as [21]

$$ST = \frac{|\max[A(i)]|^2}{|\sum_{i=1}^{N}[A(i)]^2|} \tag{17}$$

where $A(i)$ is the gray value of the ith pixel, and N is the number of pixel. As we know that communication distance affects the coupling efficiency, and the analytic relationship is [26]

$$J = 8a^2 \int_0^1 \int_0^1 \exp[-(a^2 + A_R/A_c)(x_1^2 + x_2^2)] \cdot I_0(2A_R/A_c x_1 x_2) x_1 x_2 dx_1 dx_2 \tag{18}$$

where I_0 is the modified first kind of zero-order Bessel function, $a = (D_R/2)\ (\pi W_m/\lambda f)$, $A_R = \pi D_R^2/4$, $A_c = \pi \rho_c^2$, $\rho_c = (1.46 C_n^2 k^2 L)^{-(3/5)}$, L is the communication distance, A_R is the area of the receive aperture, A_c is space coherent area of the incident wave, ρ_c is the coherent length, D_R is the aperture of the receive lens, W_m is the aperture of the mode distribution at the end of the fiber, f is the focal length of the lens, λ is the wavelength, and $k = 2\pi/\lambda$, C_n^2 is the atmospheric optical refractive index structure parameter.

4. Numeral simulations

We introduce the incident wavefront aberration with the Zernike coefficients shown in Table 1.

The intuitive introduced wavefront aberration is shown in Fig. 6. The corresponding coupling efficiency is 41.67%.

In the following numeral simulations we can see that the *RMS* value of the wavefront will decrease to a very small ending-value with the algorithms mentioned above.

We take the parameter $\eta_1 = \eta_2 = 2$ and $\omega = 1 - iter \cdot 1/MaxIter$, *iter* is the current iteration number and *MaxIter* is the maximum iteration number. The changing trends of the coupling efficiencies with different algorithms (PSO, MSFL, SFL etc.) are shown in Fig. 7. Note that 100 individuals are used in every algorithm.

From Fig. 10 we can get that MSFL does well in both convergence value (about 0.9) and convergence speed (converges at the 10th iteration). It is better than PSO (converges at the 50th iteration) in convergence speed and better than MAFS in both speed (converges at the 30th iteration) and convergence value (about 0.87).

Apparently, MSFL is better than SFL algorithm both in the convergence value and speed. They show the superiorities of MSFL

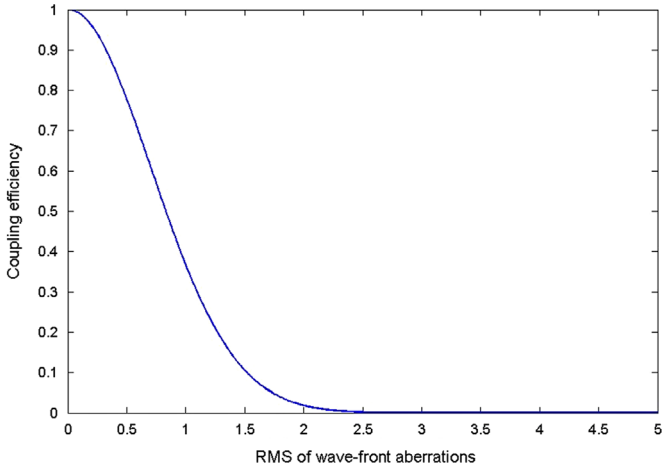

Fig. 9. Relationship between coupling efficiency and *RMS* value.

Table 2
Comparison of coupling efficiency at FSO receiver.

Initial coupling efficiency (%)	Coupling efficiency with PSO (%)	Coupling efficiency with MAFS (%)	Coupling efficiency with MSFL (%)
41.7	90.0	87.0	90.0

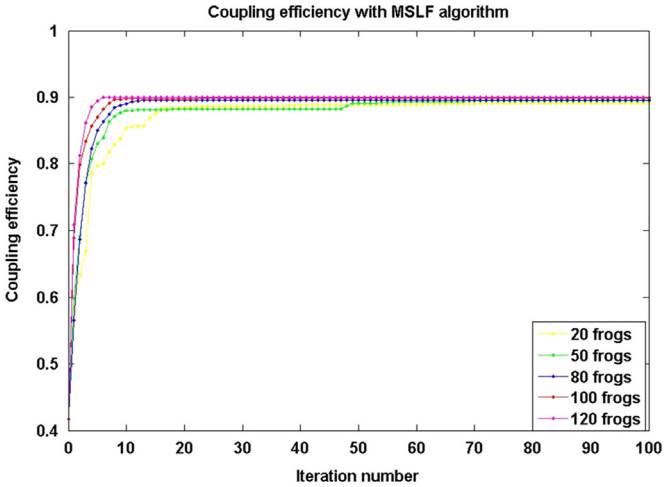

Fig. 10. Coupling efficiency with MSFL algorithm.

Table 3
Comparison of residual wavefront aberrations between different numbers of individual.

Residual wavefront after 1 iteration	Residual wavefront after 5 iterations	Residual wavefront after 100 iterations
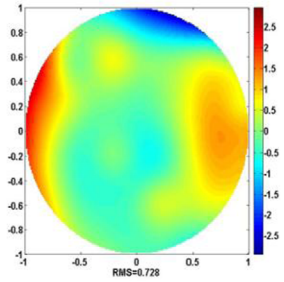	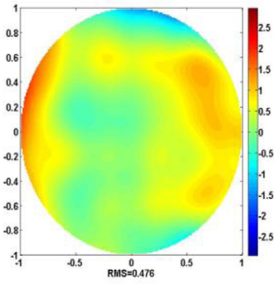	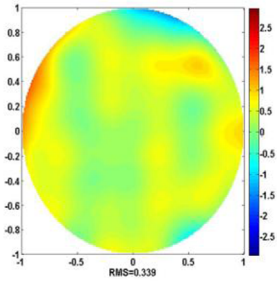
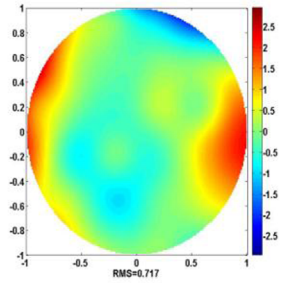	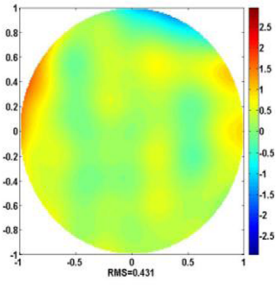	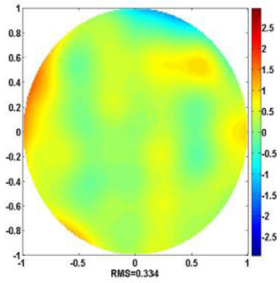
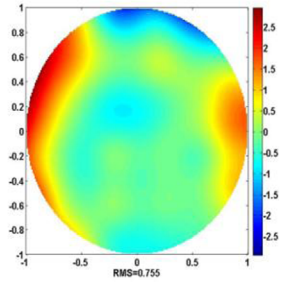	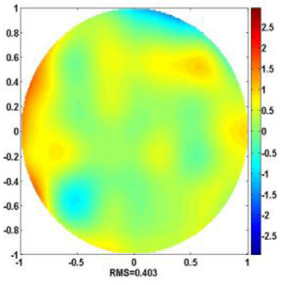	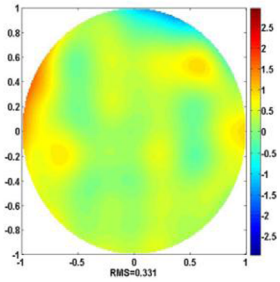
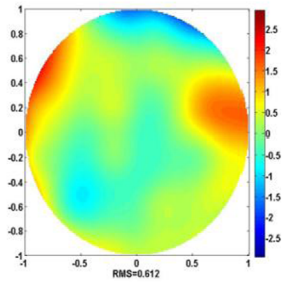	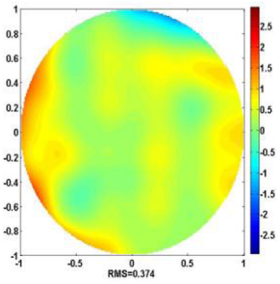	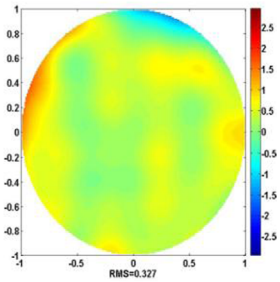
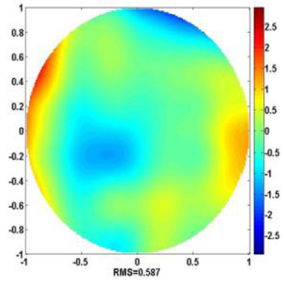	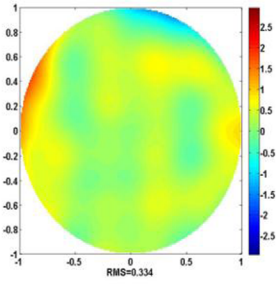	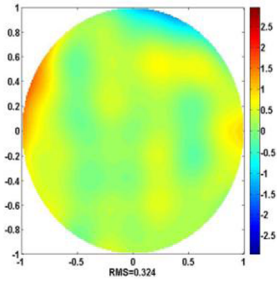

in a higher-dimensional space. The conventional SFL will converge to a local optimized solution. The residual wavefront aberrations after correction with MSFL, MAFS and PSO are shown in Fig. 8.

The *RMS* values after correction are 0.327 (MSFL), 0.371 (MAFS) and 0.322 (PSO), they are significantly reduced. We can easily see that the wavefront aberrations after correction are more smooth than the incident wavefront. That means these algorithms are very effective.

MSFL algorithm has the best overall capability of compensating the wavefront aberration. From Eq. (15) we get that the smaller *RMS* value of the wavefront aberration leads to the higher coupling efficiency. The numerical relationship between them is shown in Fig. 9.

Detailed data of coupling efficiency of PSO, MAFS and MSFL is shown in Table 2.

Use 20, 50, 80, 100 and 120 frogs respectively to show the effect of MSFL algorithm on the coupling efficiency in the FSO communication system. In each experiment the frogs are separated in 5 groups by grouping operation. The coupling efficiency is shown in Fig. 10.

It is easy to get that the theoretical limit of MSFL algorithm is largely fixed. Therefore we can get the conclusion that the convergence value is stable but the convergence rates are very different. When 20 frogs exist, the searching process begins to converge at the 20th iteration. When 50 frogs exist, the performance is worse and the local optimization tends to occur. With the increased number of individuals the rate is higher, the process begins to converge at the 15th (80 frogs), 10th (100 frogs) and 5th (120 frogs) iteration. The reason is that the more the individuals, the better searching ability the algorithm has.

To make it more direct, the initial wavefront aberration and residual wavefront aberrations after 1, 5, 100 iterations are shown in Table 3. Each row respectively shows the results of 20, 50, 80, 100, and 120 frogs.

The conclusion is in line with Fig. 10.

In MSFL algorithm, the whole individuals should be assigned to many groups. Here we give some discussions on the effects of different group numbers on the coupling efficiency. We set 100 frogs in the solution space and assigned them to 1, 4, 10, 20, 25,100 groups respectively, and then the corroding frog-number in each group is 100, 25, 10, 5, 4, 1. The simulation result is shown in Fig. 11.

Different group numbers leads to different results. Neither too many nor too few groups get a good result. In our simulations, the best compensation occurs when the frogs are in 4 groups. This means the MSFL algorithm largely depends on the group number, if it is too large, the frogs in every group is not enough, thus the advantage of the "local searching" disappears. If the group number is too small, the searching procession will be trapped in the local extremum. In practice, the group number should be selected by the specific conditions and after many times tests and design modification.

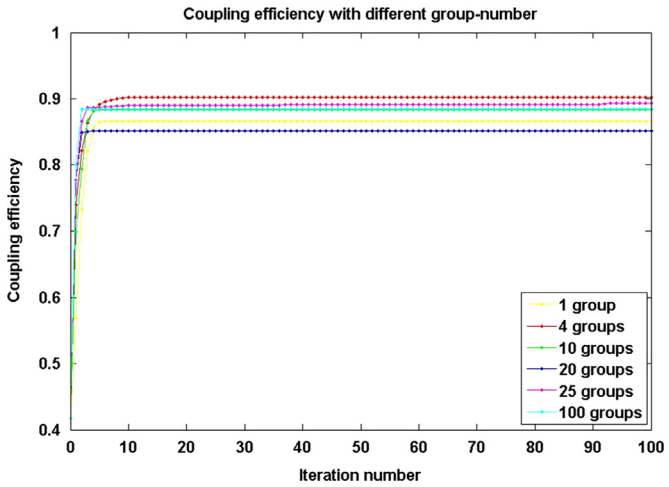

Fig. 11. Coupling efficiency with different group number.

Take some numeral simulations to compare the difference between ABCA and SPGD in convergence characters. In the simulations, ε is determined by the disturbance in iteration, C is 0.8. and γ_0 is chosen according to the test results. Some coupling efficiencies with different γ_0 are shown in Fig. 12.

It is obvious that SPGD can converge better in a slow convergence speed. With the prerequisites described in this study (parallel off line computing elements), MSFL needs only 7–10 iterations to get a relatively good value (90.0%, 100 frogs), but SPGD needs hundreds of iterations. In the comparison of the proposed algorithms, we setup an experimental FSO communication system and use SPGD, PSO and MSFL algorithm for close-loop compensating atmospheric turbulence. In this system, the chosen parameters are presented in Table 4.

We evaluate these algorithms in experiments of simulation analysis in which the result tendencies are generally same. The intensity distributions are shown in Table 5 (each row in the table represents MSFL, PSO and SPGD algorithm respectively). The initial coupling efficiency is about 5–6% which seriously affects the performance of the system. Compared with SPGD, MSFL first offers better coupling efficiency value (about 50 iterations, coupling efficiency 66.2%), and PSO reaches its convergence value. But SPGD does not get good value even after 80 iterations (only about 48%). Getting the appealing effects like the results in simulation is almost impossible. In general, the final value in real experiment can only achieve more than 60%. There are several reasons for this, for example, the noise within the system, limitation in processer speed, the poor stability of DM etc. The noise in the system should be restrained by using better electronic components to reduce the thermal noise. Faster processer could be used to control DM so that the instantaneity of the system will be better. And the most important reason is the DM stability, which means that DM should generate the identical corrected phase by the same voltage applied on the actuators in theory. But in practice it is limited by the processing craftsmanship, so how to get DM with high stability is a significant engineering problem. But the improvement in images is significant and the light scintillation is eased (shown at the top right

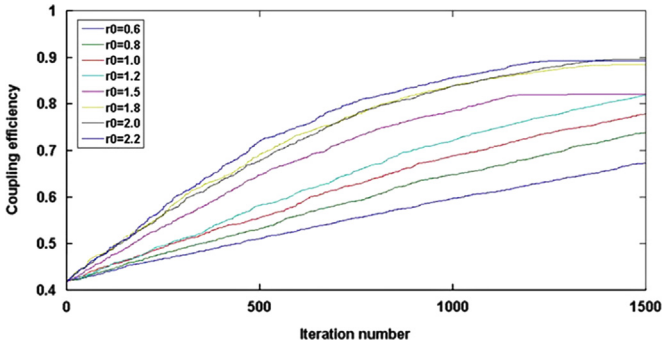

Fig. 12. Coupling efficiencies based on SPGD with different γ_0.

Table 4
Parameters in the FSO system.

Parameter	Value
Diameter of transmitter (mm)	20
Diameter of receiver (mm)	20
Laser wavelength (nm)	532
Deformable mirrors unit number	32
Pixel size of CCD camera (μm)	5
Resolution of CCD camera	1024 × 1024
Frames per second of CCD camera	1076

Table 5
Result in the experiment system.

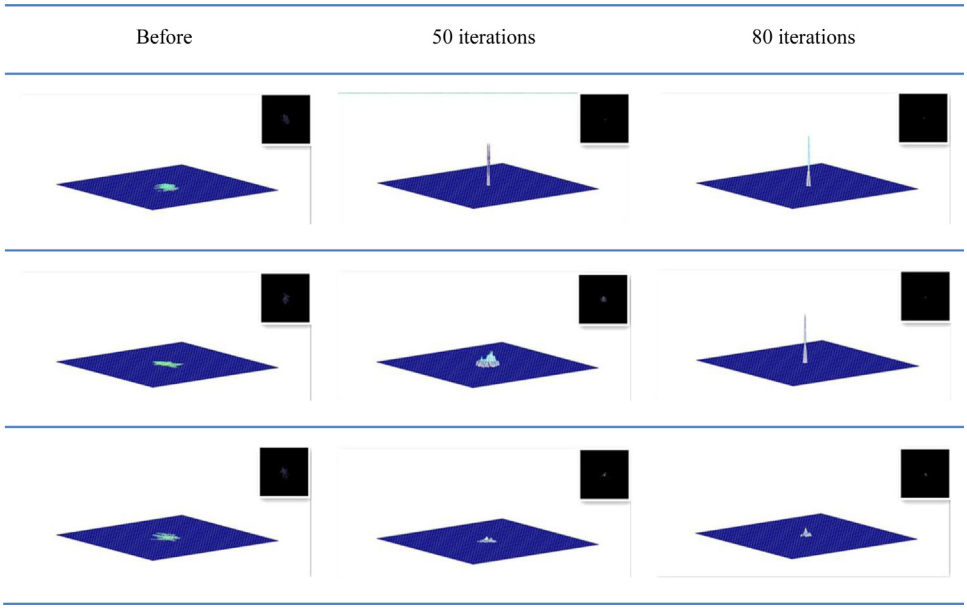

corner of each image). It makes sense in some important circumstances such as Military Satellite Communications etc.

5. Conclusion

In this paper, in order to make the FSO communication system work steadily under the bad atmospheric environment, a sensor-less FSO AO system with MSFL is proposed to compensate the wavefront aberration. Since MSFL algorithm has better convergence property, the AO–FSO system can get better performance. Some groups of comparisons simulations and experiments between MSFL and PSO, SPGD have shown that MSFL algorithm performs well in the wavefront aberration compensation. With parallel process technology, MSFL converges faster, which is especially important to the real-time of the FSO system. The performance analysis of the FSO communication system shows that the average coupling efficiency increases (from 41.67% to about 90%, in the experiments it achieves about 65%), and the dissipation of energy is reduced.

Acknowledgment

This work was supported by the National Natural Science Foundation of China (No. 61171079).

References

[1] Mohammad Abtahi. Suppression of turbulence-induced scintillation in free-space optical communication systems using saturated optical amplifiers. IEEE J Lightwave Technol 2007;24(12):4966–73.
[2] Liu Wei, Wenxiao Shi. Free space optical communication performance analysis with focal plane based wavefront measurement. Opt Commun 2013;309:212–20.
[3] Chen Yuhui, Huang Lu, Gan Lin, Zhiyuan Li. Wavefront shaping of infrared light through a subwavelength hole. Light: Sci Appl 2012;1(e26):1–5.
[4] Douglas P Looze. Structure of LQG controllers based on a hybrid adaptive optics system model. Eur J Control 2011;3:237–48.
[5] Poyneer Lisa, Véran Jean-Pierre. Predictive wavefront control for adaptive optics with arbitrary control loop delays. J Opt Soc Am A 2008;25(7):1486–96.
[6] Liu Chao, Hu Lifa. Modal prediction of atmospheric turbulence wavefront for open-loop liquid-crystal adaptive optics system with recursive least-squares algorithm. Opt Commun 2012;285(3):238–44.
[7] Schwarz Jens, Ramsey Marc. Low order adaptive optics on Z-Beamlet using a single actuator deformable mirror. Opt Commun 2006;264(1):203–12.
[8] Fedrigo Enrico, Muradore Riccardo, Zilio Davide. High performance adaptive optics system with fine tip/tilt control. Control Eng Pract 2009;17(1):122–35.
[9] Mikhail Vorontsov A. Decoupled stochastic parallel gradient descent optimization for adaptive optics: integrated approach for wavefront sensor information fusion. J Opt Soc Am 2002;19(2):356–68.
[10] Guilin Liu, Huafeng Yang. Experimental verification of combinational deformable mirror for phase correction. Chin Opt Lett 2007;5(10):559–62.
[11] Mooseok Jang, Anne Sentenac, Changhuei Yang. Optical phase conjugation (OPC)-assisted isotropic focusing. Opt Express 2013;21(7):8781–92.
[12] Monir Morshed, Lowery Arthur J, Du Liang B. Improving performance of optical phase conjugation by splitting the nonlinear element. Opt Express 2013;21(4):4567–77.
[13] Weyrauch Thomas, Mikhail Vorontsov A. Atmospheric compensation with a speckle beacon in strong scintillation conditions: directed energy and laser communication applications. Appl Opt 2005;44(30):6388–401.
[14] Buffington A, Crawford FS, Muller RA, Schwemin AJ, Smits RG. Correction of atmospheric distortion with an image-sharpening telescope. J Opt Soc Am 1977;67(3):298–303.
[15] McCall SL, Brown TR, Passner A. Improved optical stellar image using a real-time phase-correction system: initial results. Astrophys J 1977;211:463–8.
[16] Hardy JW. Active optics: a new technology for the control of light. Proc IEEE 1978;66:651–97.
[17] O'Meara TR. The multidither principle in adaptive optics. J Opt Soc Am 1977;67:306–15.
[18] Pearson JE, Hansen S. Experimental studies of a deformable-mirror adaptive optical system. J Opt Soc Am 1977;67:325–33.
[19] Bifano TG, Perreault J, Bierden PA. Micromachined deformable mirrors for adaptive optics. Proc SPIE 2002;4825:10–3.
[20] Hinchey MG, Sterritt R, Rouff C. Swarms and swarm intelligence. IEEE Comput 2007;40(4):111–3.
[21] Kennedy, J, Eberhart, R. Particle swarm optimization. In Proceedings of the IEEE international conference on neural networks, 1995; 4: p. 1942–1948.
[22] Kennedy, J, Eberhart, R. A new optimizer using particle swarm theory. In Proceedings of the IEEE sixth international symposium on micro machine and human science; 1995.
[23] Chen Ying, Feng Yong, Xinyang Li. A parallel system for adaptive optics based on parallel mutation PSO algorithm. Optik 2014;125(1):329–32.
[24] Sabry Yasser M, Saadany Bassam, Khalil Diaa, Bourouina Tarik. Silicon micromirrors with three-dimensional curvature enabling lensless efficient coupling of free-space light. Light: Sci Appl 2013;2(e94):1–9.
[25] Weyrauch Thomas, Vorontsov Mikhail A. Fiber coupling with adaptive optics for free-space optical communication. Proc SPIE 2002;4489:177–84.
[26] Yamac D, Frederic MD. Fiber-coupling efficiency for free-space optical communication through atmospheric turbulence. Appl Opt 2005;44(23):4946–52.